Radial infall of pebbles and dust pile-up at the ice line in a protoplanetary disk

Erik Jeppsson

Lund Observatory
Lund University

2013-EXA77

Degree project of 15 higher education credits
November 2013

Supervisor: Anders Johansen

Lund Observatory
Box 43
SE-221 00 Lund
Sweden

Radial infall of pebbles and dust pile-up at the ice line in a protoplanetary disk

Erik Jeppsson

Supervisor: Doc. Anders Johansen

Lund University

Abstract

We investigate the radial infall of ice pebbles in a protoplanetary disk, and how these tend to end up in relatively close proximity to eachother, providing a possible spawning ground for planets. These pebbles have dust particles embedded in them, which are released as the pebble crosses the so-called ice-line, where the ice evaporates. This is interesting as the dust will pile up around this ice line and possibly form planets over time. A simple model of the radial infall is set up, using the programming language IDL, and evidence of this dust pile-up at the ice line is shown. We use an ice-line situated at 3 AU, and the Minimum Mass Solar Nebula equations of Hayashi. We find that the test particles do indeed collect inside the radius of 3 AU after an elapsed time of $10^5 - 10^6$ years. We also find that the streaming instability mechanic is a probable culprit in attaining high particle density.
Finally, we correlate the results with the currently known exoplanets, and find that the thus far detected exoplanets seem to exist in close proximity to their respective stars, inside their ice-line radius.

I. Introduction

Any model needs an experimental basis and planet formation is no different. This is a bigger problem, perhaps, than most other areas of astronomy because of the small size of the objects involved, as well as their proximity to the star they orbit. We have only recently begun (indirectly) observing extrasolar planets, and then only faintly. A fluctuation in light flux of the star can be the only thing telling us that something is there. When we consider planet formation happens in a disk of material around the host star, we instantly realize how little information we have. We need a somewhat decent telescope to see the details of the rings of Saturn, and the distance from Earth to Saturn is puny in comparison to that of Earth to the nearest extrasolar star.

In the past decade there has been a boom in exoplanets being confirmed. This is mostly due to new methods and better equipment. The two main methods used (though others exist) are called the transit method and the radial velocity method. The former concerns measuring the change in intensity as a planet passes across the disk of the star. The latter means measuring the very small shifts in movement of the star, induced by the nearby planet. Combining these two methods makes for a powerful tool that can quantify both the mass and radius of an exoplanet. However, both methods have their disadvantages, most notably that the farther away from a star a planet is, the harder it is to detect. Therefore we currently have most knowledge of planets

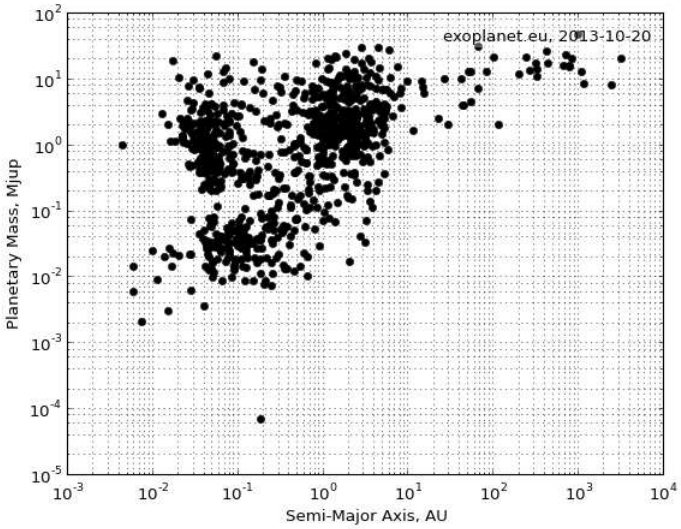

Figure 1: *exoplanet mass (m_{Jup}) as a function of the distance between exoplanet and star (AU). The largest congregation of exoplanets is situated at roughly 3 AU, but there are also aggregates closer to the respective stars. One should keep in mind that the location of the ice line is different depending on the properties of the host star. Also note that most detected stars are more massive than Earth.*

close to their host star.

As of the writing of this thesis, 999 exoplanets have been confirmed to exist, a number that will no doubt rise rapidly in the years to come. The result of these "sightings" is that astronomers now have a whole new source of data. For the study of planet formation the new data is invaluable, because it gives a hint of the structure of a planetary system that is not ours. For instance, are earth-like planets situated at 1 AU in other systems, or are we sitting on an anomaly? Are planets formed where we previously thought? Many questions will surely be answered in the near future that could not have been answered without the discoveries of exoplanetary systems.

The goal of this paper is to investigate if dust gathers close to the star, presumably forming rocky planets in its vicinity. Therefore, data showing relatively low-mass planets relatively close to the star would, on a basic level, back up the claims made later in the thesis. Such a plot can be seen in figure 1, which shows an assortment of confirmed exoplanets of low mass close to their host star (image courtesy of exoplanet.eu).

That the near vicinity of a star is a good place for planet formation comes down to a quirk in nature, the water ice line. Situated at around 3 AU in our solar system, it is the shell that divides sublimated and condensed ice. This rather sharp divide has interesting and useful effects on the trajectory of pebbles containing ice, which will be shown below. It has been shown that the near vicinity of the ice line is a good place for planet formation (Ros and Johansen (2013)). It should be remembered that the ice-line is star-specific; a hotter star will have its ice line further out in the system. This means that planets would form, generally, further out.

The study of planet formation is tricky, since we cannot see it progress. What we can do is to backtrack, to reverse-engineer our own solar system, which was presumably once created the same way as all other systems. The theory for this reverse-engineering method was laid down in the 1970's, and is explained in the Minimum Mass Solar Nebula section, below.

The formation of planets is a dynamic process, and modelling the creation process from clouds of gas and dust is a very difficult task and not all processes involved are yet understood. Currently, most models indicate that meter-sized objects and above ought to evaporate as it gets too close to the star it orbits, or get shattered into smaller pieces as they collide against eachother. These are hurdles that need to be overcome to get the true, physical picture of reality in these planetary disks. This work, however, is a toy model of the inward radial drift that occurs for grains in a disk, and these hurdles will be disregarded.

Planet formation starts from small dust grains in the protoplanetary disk around a young star. The term dust refers to solid particles, as opposed to gas, which is also present in the disk. A particle in free space would orbit around the system center of mass with the Keplerian frequency

$$\Omega_K = \sqrt{\frac{GM_\star}{r^3}} \tag{1}$$

where G is the gravitational constant, $M_\star$ the mass of the star, and r the distance from the star.

However, protoplanetary disks also contain gas, which moves with sub-Keplerian speeds. There is a pressure gradient and a temperature gradient in the disk, meaning that the inner portions of a disk is denser, and thus has both higher pressure and temperature than the outer disk. Like any rotating thing, the gas feels a centrifugal force from its orbit. This force is however in balance with the gravitational force exerted on the gas from the star. The pressure and temperature gradients makes the gas molecules feel a decrease in gravitational pull from the star, making the whole gaseous part of the disk orbit slower than the Keplerian speed.

The slow-moving gas forces the solid pebbles to move below the Keplerian speed. This will make the pebbles lose angular momentum and thus fall inwards, toward the star. This inwards drifting takes place over an extended period of time, so the real motion is a spiralling one. It can however be easier to imagine as a straight inwards drift if we adapt a frame of reference that is co-moving with the pebble in question. As they drift, the pebbles collide with eachother and, depending on their sizes, will merge, bounce off eachother, or be left shattered *(Zsom, A.; Ormel et al. (2010)*).

II. The MMSN

We cannot directly investigate the small-scale dust formations around young stars, or how small grains eventually clump together and finally form planetesimals. Therefore it is prudent to form a model of these events. However, we do not know the mass distribution in planetary disks either. This prompted Weidenschilling (in 1977) and Hayashi (in 1981) to construct an empirical model of the initial mass-conditions of our own solar system, the Minimum Mass Solar Nebula, or MMSN. This is a model nebula with the minimum amount of mass needed to form the solar system. It consists of a set of equations that give various important variables, such as density and temperature, often as a function of radial distance from the star. The term *minimum mass* indicates that all the mass of the nebula is accreted onto the planets, none being lost to space.

The MMSN is made up by dust alone. The dust to gas ratio is assumed to be 0.01, so to get an understanding of the gas we simply multiply by 100.

The MMSN used in this work is the one of Hayashi (1981). It is an early model and is likely outdated, but as this paper presents a toy model, it is sufficient for our purposes.

II.1 The equations

The temperature T as a function of distance r from the central star, is given by

$$T(r) = 280K \left(\frac{r}{\text{AU}}\right)^{-\frac{1}{2}} \tag{2}$$

A plot of this relation for a disk of radius 100 AU can be seen in figure 2-A. It should be noted that the temperature given here is for the simple case where all the heat comes from radiation from the central star (i.e. no extrasolar radiation or viscous heating).

The column density, the mass of an area integrated over some distance, is given by

$$\Sigma(r) = \Sigma_0 \left(\frac{r}{\text{AU}}\right)^{-\delta} \tag{3}$$

The Hayashi MMSN uses the exponent $\delta = \frac{3}{2}$.

Thus

$$\Sigma(r) = 1700 \text{ g cm}^{-2} \left(\frac{r}{\text{AU}}\right)^{-\frac{3}{2}} \tag{4}$$

The value 1700 g cm^{-2} comes from taking all the solid matter in the planets and spreading it between their orbits.

The isothermal speed of sound, i.e. the speed of accoustic waves in the disk medium, is for our MMSN given by

$$c_s = \sqrt{\frac{kT}{\mu}} = 9.9 \cdot 10^4 \sqrt{\frac{T}{280K}} \tag{5}$$

where k is Boltzmann's constant and μ the mean molecular weight.

With this we can calculate the scale height of the disk. The scale height is the distance over which a quantity, here pressure, decreases by e.

$$H(r) = \frac{c_s}{\Omega_K} \tag{6}$$

The relation between H and r can be seen in figure 2-C.

A disk is not uniformly thick as it extends outwards, but flares (i.e. becomes thicker) the further out we look. To find an equation for the gas density in the disk, we start with the equation of motion for the gas. If z is the height above the disk mid-plane, we have

$$\frac{dV_z}{dt} = -\Omega_K^2 z - \frac{1}{\rho}\frac{dP}{dz} \tag{7}$$

where P is the gas pressure. If we assume isothermal conditions (constant temperature), the gas pressure can be rewritten as $P = c_s^2\rho$. Assuming constant sound speed c_s, we have

$$\frac{dV_z}{dt} = -\Omega_K^2 z - c_s^2\frac{1}{\rho}\frac{d\rho}{dz} \tag{8}$$

For hydrostatic equilibrium (net velocity field is zero), we write

$$\frac{dV_z}{dt} = 0 = -\Omega_K^2 z - c_s^2\frac{1}{\rho}\frac{d\rho}{dz} \tag{9}$$

Rewriting

$$-z\frac{\Omega_K^2}{c_s^2} = \frac{1}{\rho}\frac{d\rho}{dz} \Rightarrow -z\frac{\Omega_K^2}{c_s^2} = \frac{d\ \ln\rho}{dz} \tag{10}$$

Substituting for H, using equation 6, yields

$$-\frac{z}{H^2} = \frac{d\ \ln\rho}{dz} \tag{11}$$

The solution to this is

$$\ln\rho = \ln\rho_0 - \frac{z^2}{2H^2} \tag{12}$$

Thus, the vertical density structure of the disk is given by

$$\rho(z) = \rho_0 \exp\left(\frac{-z^2}{2H(r)^2}\right) \tag{13}$$

where $\rho_0 = \rho(z=0)$ is the mid-plane density:

$$\rho_0 = \frac{\Sigma(r)}{\sqrt{2\pi}H(r)} \tag{14}$$

The final, r- and z-dependent density equation is

$$\rho(r,z) = \frac{\Sigma(r)}{\sqrt{2\pi}H(r)} \exp\left(\frac{-z^2}{2H(r)^2}\right) \tag{15}$$

The density as a function of r can be seen in figure 2-B.

As mentioned earlier, the solid particles in the disk want to orbit with the Keplerian speed, but feels a headwind from the slower-moving gas, causing the particles to spiral inwards to attain the desired speed. To get an understanding of the relative speed between these, we balance the forces acting on a solid particle in the disk in the radial direction.

$$\frac{V_\psi^2}{r} = \frac{GM_\star}{r^2} + \frac{1}{\rho}\frac{\partial P}{\partial r} \tag{16}$$

where $\frac{V_\psi^2}{r}$ is the outwards centrifugal force, $\frac{GM_\star}{r^2}$ the inwards gravitational force, and $\frac{1}{\rho}\frac{\partial P}{\partial r}$ the outwards pressure gradient force. V_ψ is the velocity in the orbital direction.

Pressure can be rewritten as $P = \rho c_s^2$.

$$\frac{1}{\rho}\frac{\partial P}{\partial r} = \frac{c_s^2}{P}\frac{\partial P}{\partial r} \tag{17}$$

multiplying by $\frac{r}{r}$ gives

$$\frac{c_s^2}{P}\frac{\partial P}{\partial r}\frac{r}{r} = \frac{c_s^2}{r}\frac{\partial\ lnP}{\partial\ \ln r} \tag{18}$$

$$\frac{V_\psi^2}{r} = r\Omega_{gas}^2 = \frac{GM_\star}{r^2} + \frac{c_s^2}{r}\frac{\partial\ lnP}{\partial\ \ln r} \tag{19}$$

Next we divide by r. Since $\Omega_K = \sqrt{\frac{GM_\star}{r^3}}$, we can rewrite eq.19 as

$$\Omega_{gas}^2 = \Omega_K^2 + \frac{c_s^2}{r^2}\frac{\partial\ lnP}{\partial\ \ln r} \tag{20}$$

We use the relation $H = \frac{c_s}{\Omega_K} \Rightarrow c_s = H\Omega_K$.

$$\Omega_{gas}^2 = \Omega_K^2 + \frac{H^2\Omega_K^2}{r^2}\frac{\partial\ lnP}{\partial\ \ln r} \tag{21}$$

Rearranging gives

$$\Omega_{gas}^2 - \Omega_K^2 = \frac{H^2 \Omega_K^2}{r^2} \frac{\partial\ lnP}{\partial\ \ln r} \tag{22}$$

Next, we divide by Ω_K^2.

$$\frac{\Omega_{gas}^2}{\Omega_K^2} - 1 = \frac{H^2}{r^2} \frac{\partial\ lnP}{\partial\ \ln r} \tag{23}$$

Looking at the left-hand side, we realize that these frequencies can be written as velocities.

$$LH : \frac{\Omega_{gas}^2}{\Omega_K^2} - 1 = \frac{v_{gas}^2}{v_K^2} - 1 \tag{24}$$

The gas moves slower than the Keplerian, so the relative speed can be written as $\Delta v = v_K - v_{gas} \Leftrightarrow v_{gas} = v_K - \Delta v$.

$$LH : \left(\frac{v_K - \Delta v}{v_K}\right)^2 - 1 = \left(1 - \frac{\Delta v}{v_K}\right)^2 - 1 \tag{25}$$

Expanding yields

$$LH : \left(1 - \frac{\Delta v}{v_K}\right)^2 - 1 = 1^2 - 2\frac{\Delta v}{v_K} + \frac{\Delta v^2}{v_K^2} - 1 = -2\frac{\Delta v}{v_K} + \frac{\Delta v^2}{v_K^2} \tag{26}$$

We assume that $\Delta v \ll v_K$, and thus

$$LH = -2\frac{\Delta v}{v_K} \tag{27}$$

Looking back at the entire equation

$$-2\frac{\Delta v}{v_K} = \frac{H^2}{r^2} \frac{\partial\ lnP}{\partial\ \ln r} \tag{28}$$

Isolating the desired end product

$$\Delta v = -\frac{1}{2}\frac{H^2}{r^2}\frac{\partial\ lnP}{\partial\ \ln r}v_K \tag{29}$$

We use the relation $\frac{H}{r} = \frac{\frac{c_s}{\Omega_K}}{\frac{v_K}{\Omega_K}} = \frac{c_s}{v_K}$ to arrive at the final equation

$$\Delta V = -\frac{1}{2}\frac{H(r)}{r}\frac{\partial\ \ln P}{\partial\ \ln r}\ c_s \tag{30}$$

To find out what $\frac{\partial\ \ln P}{\partial\ \ln r}$ is in out disk, we figure out how the pressure P depends on the distance r. We do this by looking at the r-dependencies of the other quantities.

$$\Sigma(r) = r^{-\frac{3}{2}} \tag{31}$$

$$T(r) = r^{-\frac{1}{2}} \tag{32}$$

$$C_s = T^{\frac{1}{2}} = r^{-\frac{1}{4}} \tag{33}$$

$$\Omega_K = \sqrt{\frac{1}{r^3}} = r^{-\frac{3}{2}} \tag{34}$$

$$H = \frac{C_s}{\Omega_K} = \frac{r^{-\frac{1}{4}}}{r^{-\frac{3}{2}}} = r^{-\frac{1}{4}} \cdot r^{\frac{3}{2}} = r^{\frac{5}{4}} \tag{35}$$

$$\rho = \frac{\Sigma(r)}{H(r)} = \frac{r^{-\frac{3}{2}}}{r^{\frac{5}{4}}} = r^{-\frac{3}{2}} \cdot r^{-\frac{5}{4}} = r^{-\frac{11}{4}} \tag{36}$$

So, P relates to r as

$$P = \rho\ C_s^2 = r^{-\frac{11}{4}} \cdot \left(r^{-\frac{1}{4}}\right)^2 = r^{-\frac{13}{4}} = r^{-3.25} \tag{37}$$

Finally, we arrive at our equation for ΔV:

$$\Delta V = -\frac{1}{2}\frac{H(r)}{r}\ (-3.25)\ c_s \tag{38}$$

A plot of ΔV as a function of r can be seen in figure 2-D. Peculiarly, this quantity is constant over distance.
An illustration of a protoplanetary disc can be seen in figure 3. Note that it is not a realistic depiction, scale-wise.

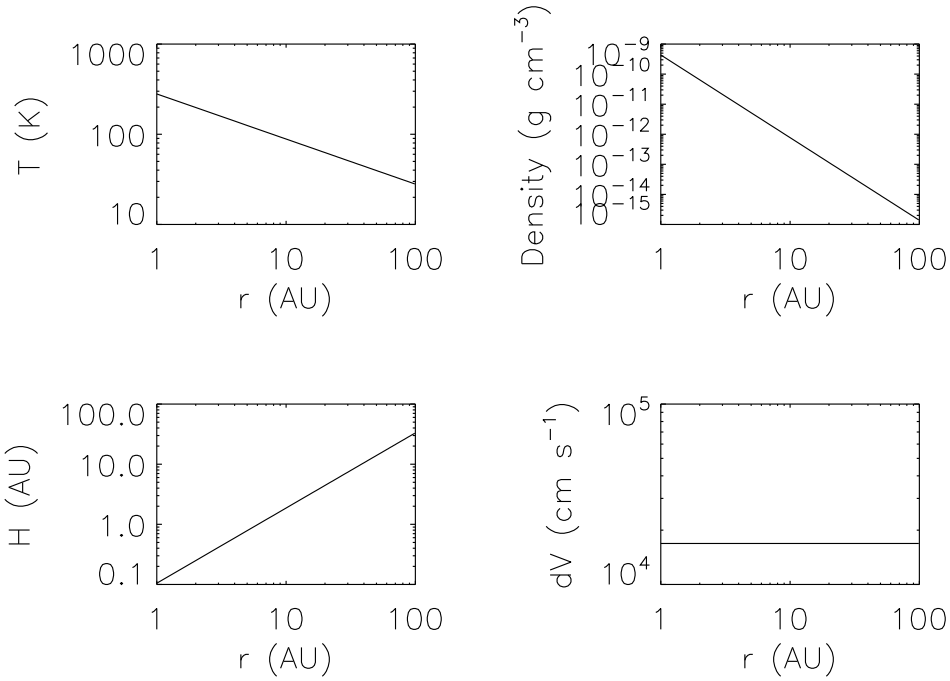

Figure 2: *The variables of the MMSN as a function of the distance from the Sun.*
A) The temperature shows that the outer disk (≈ 100 AU) has a temperature of around 30 K, while the inner disk (≈ 1 AU) has at least ten times higher temperature. At 10 AU the temperature is roughly 100 K.
B) The density is very low, $< 10^{-16} g\ cm^{-3}$ in the outer nebula, and roughly $10^{-12} g\ cm^{-3}$ at 10 AU.
C) The pressure scale height has a linear relationship to the distance in log-log.
D) ΔV, the speed difference between the Keplerian speed and the sub-Keplerian speed is curiously constant over distance.

Figure 3: *A stylized side-view of a protoplanetary disk. The Circle in the middle represents the star, and the colour gradients to the sides is a cross-section of the disk. The colour gradient indicates the pressure/temperature gradient present in the disk. Note that this is a stylized image; the relation between the star and disk is not to scale.*

III. Radial drift

The gas part of the protoplanetary disk orbits with sub-keplerian speed. The dust grains in the disk effectively feel a headwind as it tries to move past the gas. The orbits of the dust grains start to decay, and they drift inwards.

Since the protostar is a large central mass, the more massive particles in the disk will naturally feel a gravitational force inwards. The more massive the grains the larger attraction they will feel, as we know from Newton's equation of gravitation

$$F = G\frac{m_\star m_g}{r^2} \tag{39}$$

where m_g is the mass of the dust grain.

The time-scale of the radial infall is of course of interest. The time elapsed before the particle feels friction from the gas, the *particle stopping time*, is given by

$$\tau_s = \frac{a\ \rho_D}{c_s\ \rho} \tag{40}$$

where a is the particle size and ρ_D is the internal density of the particle in g cm^{-3}.

We define the drift speed of the particle as

$$V_r = -\frac{2\ \Delta v}{\Omega_K \tau_s + (\Omega_K \tau_s)^{-1}} \tag{41}$$

Weidenschilling (1977)

where $\Omega_K \tau_s$ is a dimensionless quantity called the Stokes number, which is much used in the study of protoplanetary disks. The equation is valid in the so-called Epstein regime (size of grain $\ll$ gas molecule mean-free path), wherein certain drag force laws are valid. In this regime a grain will slowly fall inwards. Conversely, in the Stokes regime (size of grain $>$ gas molecule mean-free path) a grain is large enough to have its own inclined orbit, and will thus oscillate relative to the height axis, on a much smaller time-scale than the slow infall of grains in the Epstein regime.

Knowing both the drift velocity and the distance to the star gives us the time-step to use in our calculations, $\frac{r}{V_r}$.

At a certain distance from a star is a natural boundary dubbed the water ice line. This is where the radiation heat from the star is high enough for water ice to sublimate. This will of course have dramatic consequences for any aggregate of matter containing such ice, since the previously bound, solid object loses its integrity and shatters (*Lecar, Podolak, Sasselo and Chiang (2006)*). In our simple model, this translates into aggregates of any size suddenly becoming 0.1 mm in size at the ice line, situated at 3 AU. This simulates the vanishing of the icy parts of dust clumps. In reality the change is of course less immediate and the final size of the left-over dust clumps impossible to predict.

III.1 Grain growth and aggregation

The ideas about how dust goes from free μm-sized motes to meter- and kilometer-sized objects are many, and the experiments that can be performed here on Earth are limited. Below, some of the hottest theories are detailed.

III.1.1 Sticking

What variables matter when two grains collide, and what happens? To answer these questions many experiments have been conducted by quite simply colliding objects of different compositions. Not surprisingly, the main variables at play are the sizes of the grains, their porosities, and the impactor speed. Zsom et al. (2010) put together a list of possible outcomes, depending on the interplay of these variables, from the collision of two grains. These outcomes cover sticking through surface effects, sticking by geometrical means (such as a small grain burrowing itself into a larger body), or by sticking by mass transfer. But there are also destructive outcomes, such as bouncing with mass transfer or fracture, or outright fragmentation. These latter outcomes are of course negative for planet formation.

A general result found by the study was that a particle speed below 1 m/s favours sticking, while a speed above 1 m/s would favour fragmentation of one or both of the grains.

III.1.2 Streaming instability and pressure bumps

Sticking covers what happens when the grains come into contact, but not what brought them into contact. In a fully isotropic sphere with particles strewn out, there is little direct contact. There needs to be some mixing. Various methods of mixing has been extensively modelled and simulated in the recent past, and show promise of explaining the complex process that is the creation of planetesimals from scattered dust. The goal is to get high enough concentrations to initiate gravitational collapse, which would form an object that by itself attracted surrounding material, through its gravitational pull.

Mechanical models tell us that particles in orbit will eventually fall towards the mid-plane of the disk around the rotational axis. It has been shown that this concentration of material alone is not able to initiate gravitational collapse. The solution is to think in terms of turbulence. One notion is the creation of pressure bumps, or traps, at the denser parts of the disk (near the ice line is especially interesting), towards which grains fall and get trapped. (*Barge and Sommeria 1995*) This process could over time facilitate gravitational collapse and the formation of planetesimals.

Another proposed model is the so called *streaming instability*. An aggregate of dust grains will locally reduce the head wind from the gas. Nearby solids will flow into the drafting zone behind the aggregate, since it is the place of least resistance against the gas head-wind. An analogous phenomenon is the v-shaped flight pattern of birds (*Youdin and Goodman (2004)*).

The streaming instability has been shown to be strongly dependent on metallicity *(Johansen,*

Youdin, and Mac Low (2009)). Metallicity can be equated to the abundance of condensable materials in relation to abundance of gas in the disk. Thus, pebbles with a large dust part stand a better chance to take part in streaming instabilities than otherwise. Modern MMSNs propose a condensable materials abundance of $Z \approx 0.015$, meaning that this is about what we should end up with. An initial condensable materials abundance could be $Z = 0.005$, meaning that at least a three-fold increase is needed to support the presence of streaming instability. We will look for this increase after the simulations are run.

IV. Modelling the radial drift

With the structure of the disk well described by the MMSN, we can start setting up test particles that we let fall from the outskirts of the disk into the center. As these drift inwards we will be able to see how the parameters defined above change. In this work we will consider a drift distance of 100 AU. Outside the ice line, the distance from the protostar within which ice will sublimate, the particles will be ice clumps. As the particles move inside this ice line radius, which is situated in this work at 3 AU, they will reduce to swarms of microscopic dust grains as the ice bulk sublimates. With respect to our code the particles will in effect have a drastically reduced radius at this point.

IV.1 Radial drift of a single particle

In this simplest of cases, the particle size and starting distance are set. The size is 30 cm and the starting position is 100 AU from the star. The programming language IDL is used for the computation and plotting. The program is a simple time-step loop of the dynamic equations of the system. The results are shown in the figures below. Figure 4 shows the distance from the particle to the star as a function of time. It shows that it takes about 200,000 years to reach the center of the disk from its starting point 100 AU out. We note that there is nothing stopping the particle in its tracks, it would in this model collide with the star. This is obviously bad when considering our goal of planet formation.

Figure 5 shows the mid-plane density felt by the particle as it drifts inwards. In this log-log plot it is a linearly increasing as the particle gets closer. This is in tune with the pressure gradient mentioned earlier.

Depending on how far out in the disk you look, the density differs with height, i.e. the density 1 AU above the mid-plane is not necessarily the same as at the mid-plane. Figure 6 shows the density at different heights above (or below, the disk is assumed symmetrical around the disk plane) the mid-plane. From this plot we can draw the conclusion that the disk has a flaring profile, since its inner part is more compact than its outer part.

Figure 7 shows the change in drift speed of the particle as it moves inwards. The particle reaches its maximum drift speed of 53 m/s at around 3.8 AU. The drift speed is important for the probability of sticking to other objects. A high drift speed increases the probability of destructive interactions, i.e. shattering. This would indicate that the probability of destructive interaction is at its peak at around 3.8 AU from the star.

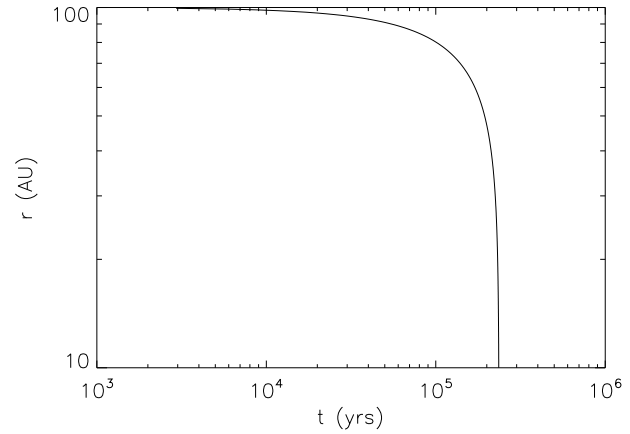

Figure 4: *A visualization of the radial drift of the single particle from 100 AU to 10 AU. The inner radius beyond 10 AU is not shown since the particle very quickly falls into the star, as the trend in the plot shows. According to our single-particle model, it takes roughly* $2 \cdot 10^5$ *years for a rock of radius 30 cm to reach the star.*

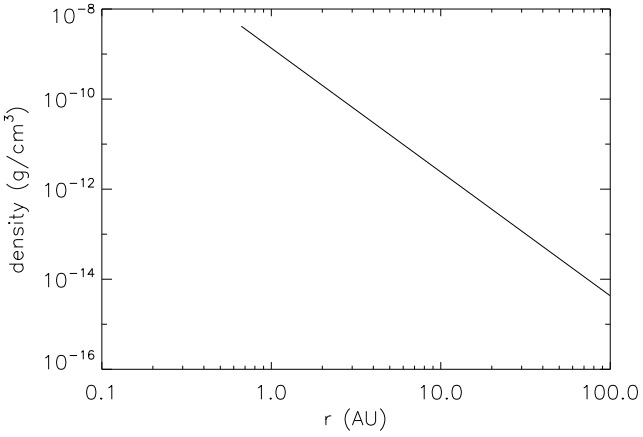

Figure 5: *The mid-plane density (z = 0) felt by the particle decreases with the radius. The plot corresponds to a particle of radius 30 cm.*

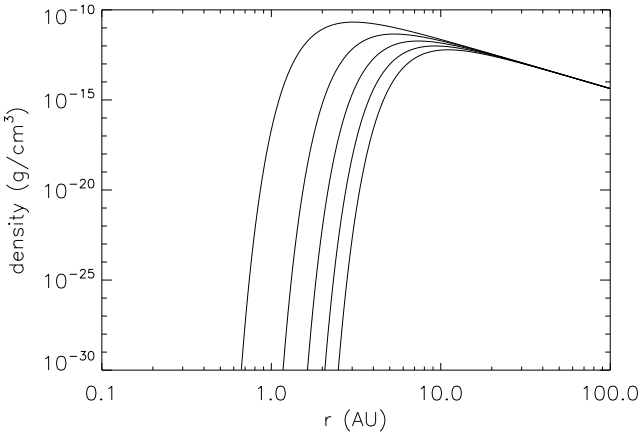

Figure 6: *Off-mid-plane densities as a function of distance to the star, corresponding to height above the plane z = 0.2 AU, 0.4 AU, 0.6 AU, 0.8 AU, and 1.0 AU. Larger heights give a cut-off further out in the disk. This is evidence that the disk is narrower closer to the star. A visual aid for this is provided in 3 below. The plots correspond to a particle of radius 30 cm.*

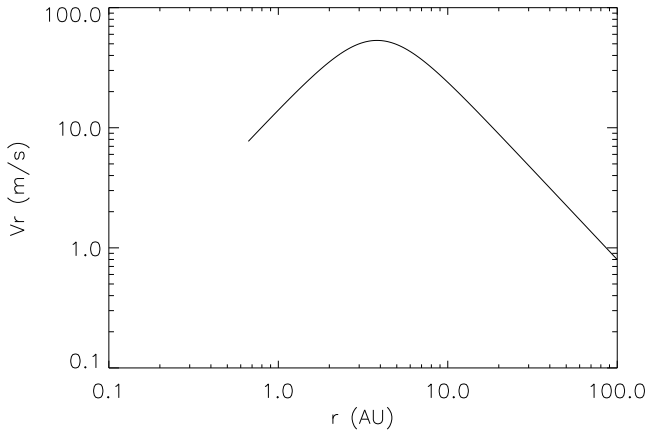

Figure 7: *The drift speed V_r as a function of distance to the star, for a single particle of radius 30 cm. The particle has its maximum drift speed of 53 m/s at $\approx$ 3.8 AU.*

IV.2 Radial drift of 100 particles

Since there is not just a single pebble in a protoplanetary disk, we are interested in what the system looks like with multiple particles. This is set up by looping not only over time-step but also over an identifying number that is assigned to each particle. This number conveys the starting radius and sizes of particles, both of which are selected pseudo-randomly from the built-in IDL command *randomu*. The number pool ranges from 0 - 100 AU for distance and 1 - 30 cm for particle sizes.

Figure 8 shows the drift of the 100 particles from 100 AU to 1 AU, as a function of time. It is clear that there is nothing stopping the particles in their tracks. In this simulation they will inevitably crash into the star.

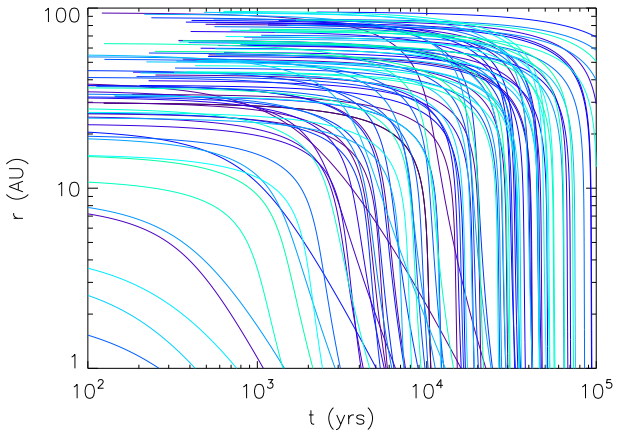

Figure 8: *The distance from the star in AU as a function of time in years. The particle radii range between 1 cm and 30 cm. The colours serve no purpose but to separate the different particles from eachother. We notice that the pebbles slowly fall inwards towards the star and never stop. This particular simulation gives no hint of any aggregation and all the particles eventually hit r=0, and thus fall onto the star.*

IV.3 Radial drift of 100 particles with ice line

Now we add an ice line at 3 AU from the star. Inside this sphere of radius 3 AU all water ice is sublimated. Most of our pebbles are made up of mostly water ice and therefore all particle sizes are reduced to μm scales once they hit this radius. This has dramatic consequences, as can be seen in figure 9. At 3 AU the particles seem to halt very sharply and all follow along a similar path. The sudden mass- and size-loss lessens both the gravitational pull and the head-wind from the gas, both of which contributed to the inwards drift. The much slower drift makes for a pile-up, much like a traffic jam where cars drive fast until they come up against the slower cars ahead.

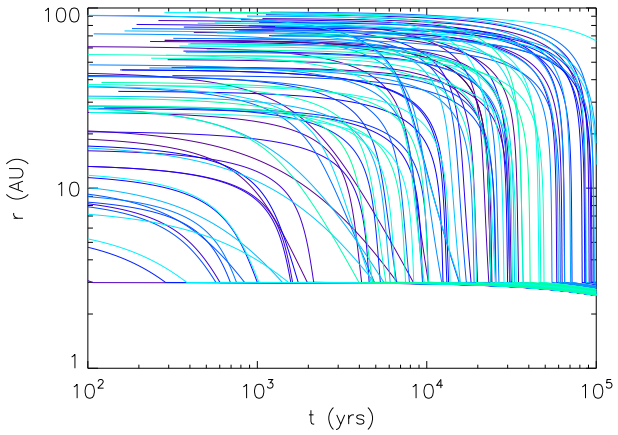

Figure 9: *The distance from the star in AU as a function of time in years with an ice line present. The effect of the ice line, situated at 3 AU, is obvious. The inwards drift of the particles suddenly decays and the particles bunch up around 3 AU. It is in this area that the density could become high enough to form localized clumps that could potentially be the seeds of protoplanets. The particle radii range between 1 cm and 30 cm.*

We see evidence of the pile-up in plots 10(a) - 10(h). These plots show the number of particles at the iceline at 3 AU and beyond (strictly < 3 AU), as a function of time. Since the initial particle size and starting location are randomized, each generated plot is different. Therefore eight plots are shown to show the overall trend. It is clear that the particles eventually settle at 3 around AU.

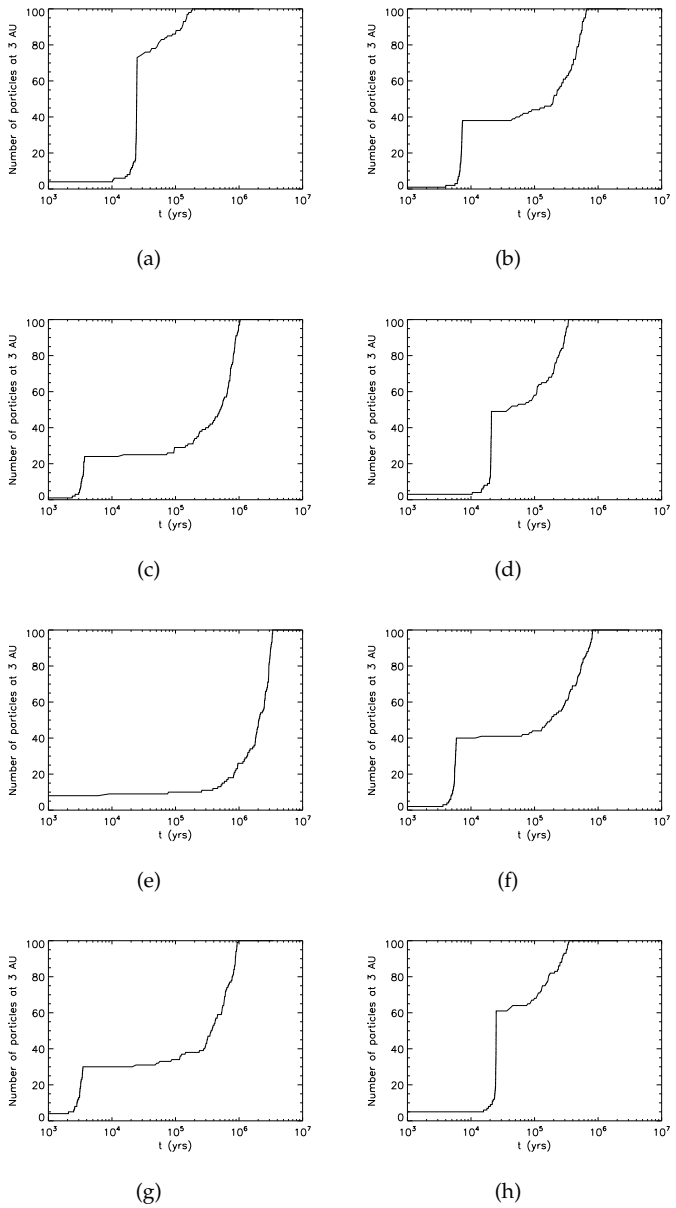

Figure 10: *Plots of number of particles at 3 AU as a function of time. There are eight plots, to better show the general trend. This is needed because of the random generation of initial position and size of the particles. The general pattern is clear; as time goes on, all 100 particles will eventually be at a distance of 3 AU from the star, the location of the iceline.*

The result we have would indicate that the density of solid, non-icy matter at and below 3 AU would eventually become high. Perhaps high enough to form planets, over time. To back up this fantastic claim, we note that within our own Solar system, the terrestrial planets are all within the ice line. A natural conclusion, then, is to assume that the pile-up of non-icy matter below the

ice line is the seed of terrestrial planet formation. Here small solid objects will grow larger by interacting with eachother constructively.

As mentioned in section III.1.2, a three-fold increase in condensable materials (i.e. dust) abundance is needed to be able to assume that the streaming instability is a factor in the planet formation process. Looking at plots 10(a) - 10(h) we see that this is the increase is $\gg 3$ in all cases, at the ice-line.

IV.4 The program

All the code used in this project was written by the author, with occasional tips from the supervisor. The code can be found in Appendix I.
The programming was done using the language IDL. Firstly the Hayashi MMSN was constructed by simply transferring the radially dependent equations found in the MMSN section above into code form. This yielded figure 2, and a general understanding of the structure and relationships of the disc.
The radial drift, initially for one particle, was simulated by running these equations over a FOR loop 1000 times. During this time the equations are iterated over and over. All the equations are related to the distance r in some manner, and r is updated at the end of each iteration. This is how we get the parameter data from the equations for each radial distance segment.
Multiple particles are added by looping the previous loop a 100 times, the selected number of particles. In the loops, the distance variable r and particle radius variable a are all made to call to the j:th element, where j is the iteration variable of the new multi-particle loop. r and a are no longer set at the beginning by the user, but randomized by IDL's *randomu* function. This for a more realistic result.
Thirdly, the iceline is implemented simply by and IF statement converting any particles with $r < 3$ AU to μm-sizes.

The parameter outputs are filed into a three-variable object of the form $output[n, i, j]$, where n specifies the parameter, eg. density. These are plotted against eachother to get the resulting figures found in this thesis.
Finally, figures 10(a) - 10(h) where produced by setting up another double FOR loop, this time with the variables of time and particle count. Inside the loop is an IF statement telling the program to add one to a counter if a particle is below 3 AU.

V. Conclusion and discussion

In this thesis we have explored the radial infall of icy pebbles in a protoplanetary disk and the effect of the ice-line on these. We find that there is a significant increase in density inside the ice-line with time. After $10^5 - 10^6$ years all 100 test particles have drifted inside the radius of the ice-line, which is set to 3 AU. A region of high density naturally lends itself well to planet creation, and to this end we have also concluded that streaming instabilities are possible as a planet formation mechanic.

In essence, we have shown in this paper that finding exoplanets within 3 AU (for solar-like stars) should be possible. If we look back at figure 1, we see that this is where most exoplanets are indeed found. However, one should keep in mind that this is not the complete picture, and that exoplanets further from their stars and/or less massive are harder to detect with current methods.

The model presented in this work is a simple one, and thus can not be seen as anything but a very rough view of reality. What is to be taken from this paper is the fact that dust particles pile up inside the ice line. The increased density means more particle-particle collisions and thus a build-up of larger solid objects. There are however major problems for the continued growth of these bodies, problems that largely are not mentioned in this work.

A few downsides of this model include:
- The motion of the particles are too predictable. The effects of f.i. turbulent diffusion could be mimicked by applying a random walk to the particles.
- The particle sizes are initially set, and the model does not allow for any particle growth.
- Each particle acts on its own, and no forces between them are taken into account.

This work could be expanded in the direction of measuring the dust density at the ice line pile-up, as well as other interesting parameter changes in this area. Adding some sort of density condition for gravitational collapse could determine the possibility of planetoid formation from the ice line pile-up alone. Finally, planet formation aids such as instabilities and pressure differences could be taken into account.

References

[1] Barge, P.; Sommeria, J. - Astronomy and Astrophysics, 295:L1-L4, 1995.

[2] Hayashi, C. - Prog. Theor. Phys. Suppl., 70, 35, 1981.

[3] Johansen, A; Youdin, A.; Mac Low, M-M. - The Astrophysical Journal, vol. 704, p. L75-L79

[4] Lecar, M.; Podolak, M.; Sasselov, D.; Chiang, E. - The Astrophysical Journal, 640:1115-1118, 2006.

[5] Ros, K.; Johansen, A. - Astronomy and Astrophysics, Volume 552, id.A137, 14 pp.

[6] Weidenschilling, S.J. - Monthly Notices of the Royal Astronomical Society, 180:57-70, 1977.

[7] Youdin, A.; Goodman, J. - The Astrophysical Journal, 620:459-469, 2005.

[8] Zsom, A.; Ormel, C. W.; Güttler, C.; Blum, J.; Dullemond, C. P. - Astronomy and Astrophysics, 513, 2010.

VI. Appendix A - The code

```
;syntax on

;————————————————————;
;       CONSTANTS       ;
;————————————————————;
;r = 100*1.49d13                ]
;a = 30                         ]-use for single particle
;time = 0                       ]
z = 0.0d*1.49d13                ;cm
M = 1.0*1.99d33
G = 6.67d-8
rhoD = 3                        ;material density

;————————————————————;
; DYNAMIC EQUATIONS ;
;————————————————————;
nt = 1000
np = 100
output = fltarr(10,nt,np)               ;for many particles

r = 3+97*randomu(seed,1,100)*1.49d13    ;random distribution of r (3-100 AU)
a = 1+29*randomu(seed,1,100)            ;random particle sizes (1-30 cm)

FOR j = 0, np-1 DO BEGIN
    time = 0
 FOR i = 0, nt-1 DO BEGIN
     T = 280*(r[j]/1.49d13)^(-1.0/2.0)
     Cs = (9.9d4)*sqrt(T/280)
     omegaK = sqrt((G*M)/(r[j]^3.0))
     H = Cs/omegaK
     dv = -0.5*(H/r[j])*(-3.25)*Cs
     sigma = 1700*(r[j]/1.49d13)^(-3.0/2.0)
     dens = (sigma/(sqrt(2*!pi)*H))*exp((-z^2.0)/(2*H^2.0))
     ts = (a[j]*rhoD)/(Cs*dens)
     Vr = -(2*dv)/((omegaK*ts)+((omegaK*ts)^(-1.0)))
     dt = abs(r[j]/Vr)*0.005

     r[j] = r[j]+Vr*dt
     IF r[j] LT 3*1.49d13 THEN a[j] = 0.01

     time = time+dt
     orbittime = 2*!pi*sqrt((r[j]^3.0)/(G*M))

     output[0,i,j] = time
     output[1,i,j] = r[j]
```

```
    output[2,i,j] = dens
    output[3,i,j] = dt
    output[4,i,j] = orbittime
    output[5,i,j] = Vr
    output[6,i,j] = dv
    output[7,i,j] = a[j]
    output[8,i,j] = ts
    output[9,i,j] = sigma
 ENDFOR
ENDFOR

;————————————————————;
;COUNTING  PARTICLES;
; 3AU, t=0 to t=end ;
;————————————————————;

counter = fltarr(nt)                ;creates array for counting particles
radCount = fltarr(nt,np)            ;creates array for position calculation
FOR varT = 0, nt-1 DO BEGIN         ;time variable
 FOR varP = 0, np-1 DO BEGIN        ;particle variable
     radCount[varT,varP] = output[1,varT,varP]/1.49d13
     IF radCount[varT,varP] lt 3.0000000 THEN counter[varT] = counter[varT]+1
 ENDFOR
ENDFOR

;————————————————————;
;    PLOT COMMANDS    ;
;————————————————————;
!p.charsize=1.5
!p.charthick = 2
!p.thick = 2
!x.thick = 2
!y.thick = 2
!p.charsize=1.5

;!p.multi=[0,2,2]     ;0=something, 2,2 = 2,2 matrix of plots

;set_plot,'ps'
;device,filename='namehere',/color,/encapsulated
;loadct,13

;————————————————————;
;         PLOTS         ;
;————————————————————;
;(uncomment to view);
;————————————————————;

;TIME VS PARTICLE COUNT AT 3AU
```

```
;plot,output[0,*,0]/31536000,counter[*], $
/xlog, xtitle='t (yrs)', $
ytitle='Number of particles at 3 AU', $
xrange=[1d3,1d7]

;TIME VS R
;plot,output[0,*,0]/31536000,output[1,*,0]/1.49d13, $
/ylog,/xlog, xtitle='t (yrs)',ytitle='r (AU)', $
xrange=[1d2,1d5],yrange=[1,100]
;FOR j = 0, np-1 DO BEGIN
;     oplot,output[0,*,j]/31536000,output[1,*,j]/1.49d13,color=j+30
;ENDFOR

;R VS DENS
;plot,output[1,*,0]/1.49d13,output[2,*,0], $
/xlog,/ylog,xtitle='log r (AU)',ytitle='log density (g/cm!U3!N)'
;FOR j = 0, np-1 DO BEGIN
;     oplot,output[1,*,j]/1.49d13,output[2,*,j]
;ENDFOR

;R VS VR
;plot,output[1,*,0]/1.49d13,abs(output[5,*,0]/100), $
/xlog,/ylog,xtitle='log r (AU)',ytitle='log Vr (m/s)'
;FOR j = 0, np-1 DO BEGIN
;     oplot,output[1,*,j]/1.49d13,output[5,*,j]/100
;ENDFOR

;a VS VR
;plot,a/100,abs(output[5,*,0]/100), $
/xlog,/ylog,xtitle='log a (m)',ytitle='log Vr (m/s)'
;FOR j = 0, np-1 DO BEGIN
;     oplot,output[1,*,j]/1.49d13,output[5,*,j]/100
;ENDFOR

;a VS ts
;plot,a/100,abs(output[8,*,0]/31536000), $
xtitle='log a (m)',ytitle='log ts (yrs)'
;FOR j = 0, np-1 DO BEGIN
;     oplot,output[1,*,j]/1.49d13,output[5,*,j]/100
;ENDFOR


;TIME VS VR
;plot,output[0,*,0]/31536000,abs(output[5,*,0]/100), $
/xlog,/ylog,xtitle='log t (yrs)',ytitle='log Vr (m/s)'
;FOR j = 0, np-1 DO BEGIN
;     oplot,output[0,*,j]/31536000,output[5,*,j]/100
;ENDFOR
```

```
;TIME VS VR
;plot,output[0,*,0]/31536000,abs(output[5,*,0]/100), $
/xlog,xtitle='log t (yrs)',ytitle='Vr (m/s)', $
xrange=[10200,10300],yrange=[1,100]
;FOR j = 0, np-1 DO BEGIN
;      oplot,output[0,*,j]/31536000,output[5,*,j]/100
;ENDFOR

;device,/close
;set_plot,'x'

end
```